JOURNAL OF MATERIALS SCIENCE **36** (2001) 3519–3524

FIB preparation of a sensitive porous catalyst for TEM elemental mapping at high magnifications

A. J. SMITH*, P. R. MUNROE‡, T. TRAN*, M. S. WAINWRIGHT*
*School of Chemical Engineering and Industrial Chemistry and ‡Electron Microscope Unit
University of New South Wales, Sydney, Australia, 2052
E-mail: p.munroe@unsw.edu.au

Doped skeletal copper catalysts, created by selective dissolution of aluminium from a copper-aluminium alloy by caustic in the presence of an additive, has been imaged at very high magnification using a TEM. The location of the additive species has been determined by elemental mapping using an attached EDS detector. Zinc resides primarily inside the copper ligaments while chromium resides on the outside of the ligaments. Since skeletal copper is highly porous and extremely sensitive, conventional TEM preparation techniques could not be used. The preparation of the TEM samples was carried out using a focussed ion beam (FIB) miller. Several methods are outlined, along with the reasons some of them were unsuccessful for this particular material. The successful result indicates this technique may be used to analyse similar skeletal materials, such as nickel, cobalt, etc., which are otherwise difficult to prepare. It may also provide a basis for high resolution imaging or elemental analysis of other porous and/or highly sensitive materials.

1. Introduction

Skeletal copper catalysts are highly porous, air-sensitive materials made by selectively dissolving aluminium from copper-aluminium alloys using caustic [1–3]. Other metals such as nickel [4] and cobalt [5] are also successful catalysts when prepared by this method, invented by Murray Raney [6, 7]. Until recently, no-one had directly imaged the internal structure of these catalysts, rather structural information was inferred from surface area analysis, x-ray and electron diffraction results [2, 8–10]. The main problems in characterising the structure arose from the small scale, the large porosity and the sensitivity of the highly dispersed metal to oxidation and/or rearrangement. However, Birkenstock *et al*. [11] used the scanning electron microscope (SEM) to image the external surface only of skeletal copper and nickel, although the image resolution was barely sufficient to see the surface structure of the coarser copper catalyst, and insufficient for nickel altogether. Szot *et al*. [12] tried using a transmission electron microscope (TEM) for examination of a carbon replica of a resin-impregnated sample, however it was difficult to interpret the results in three dimensions.

Using a focussed ion beam (FIB) miller the sample may be milled and then viewed *in situ*, penetrating through the oxide layer on the surface. Since the instrument operates under high-vacuum, the sample is protected against aerial oxidation, and since metallographic preparation is not required, structural rearrangement is minimised [13]. This method allows direct imaging of the internal structure of skeletal copper for the first time. The structure was found to consist of a uniform three-dimensional network of fine copper ligaments [13]. The FIB may be appropriate for imaging the internal structure of other similar air-sensitive, porous materials.

The addition of dopants to the preparation of skeletal copper alters the structure significantly [14, 15]. The altered structure corresponds to an increased surface area, and hence activity of the catalyst. In particular, the FIB has shown that the doped internal structure is much finer, yet retains the same basic shape as undoped specimens for both chromate and zincate additions [16, 17]. The dopants are known to be incorporated into the structure [18, 19], and it was recently shown how they become incorporated [16, 17], however it has not been possible so far to locate where the dopants reside within the structure. This is the focus of the present work.

The three-dimensional network of doped skeletal copper has a ligament radius of about 20–50 nm (Fig. 1). To locate the position of chromium oxide or zinc oxide on or within these ligaments would require elemental mapping with a resolution of the order of a few nanometres. A TEM is one of the few instruments capable of this, however electron transparent specimens must be typically 100–200 nm thick. Preparation of such sections from porous, sensitive materials like skeletal catalysts is extremely challenging. Traditional methods of TEM preparation are not suitable for this type of sample because it is far too sensitive both structurally and chemically to undergo grinding or polishing. Thinning the unleached $CuAl_2$ alloy by traditional

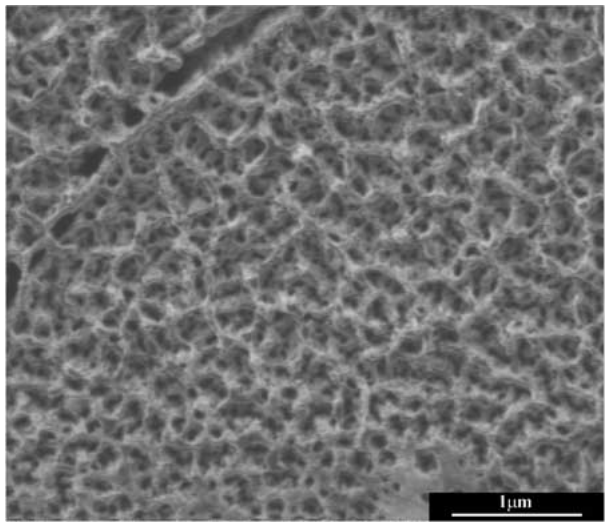

Figure 1 FIB image of the internal structure of zinc-doped skeletal copper.

electropolishing methods may remove the components in unequal amounts, thereby affecting the structural formation of the catalyst upon the leaching out of the aluminium and giving an incorrect result.

Use of a FIB for TEM preparation is a fairly new technique, although it is quickly growing in popularity [20–22]. All the previous work in this area has been with solid, structurally and chemically stable samples. This work will show several preparation methods that were tried with the FIB for the porous, sensitive skeletal copper. The aim was to obtain an elemental map of the position of both chromate and zincate in the respective doped systems. The methods tried might be applicable for elemental analysis of similar porous materials.

2. Experimental techniques

The doped skeletal copper samples were made from a 52.17wt% aluminium -copper alloy from Riverside Industrial Pty. Ltd. The alloy was re-melted and quenched to ensure homogeneity. The primary phase of this alloy was $CuAl_2$ with a small amount of Al - $CuAl_2$ eutectic, in accordance with the phase diagram [23]. The alloy was leached in 6 mol/L NaOH at 274 K overnight to remove the aluminium, leaving the porous copper. Either 0.025 mol/L Na_2CrO_4 or 0.06 mol/L Na_2ZnO_2 was also dissolved in the leaching solution as an additive.

Several methods were tried to obtain high quality samples for TEM analysis, and these will be detailed below in Section 3. Techniques that were common to all of them will be described in this Section.

Each sample was initially cut with a diamond saw to about 0.5 mm thickness. The pieces were then thinned further by grinding on 1200 grit paper to a thickness of about 50–100 μm (edge rounding begins to occur).

Thinning to electron transparency was carried out with a Philips FEI ×P200 FIB. Fig. 2 shows schematically the milling method. A "H"-type section was initially milled from the ground specimen, such that the unmilled region was about 1 μm in thickness. Further mills were then performed so that this section was thinned to an electron transparent thickness of 100 to

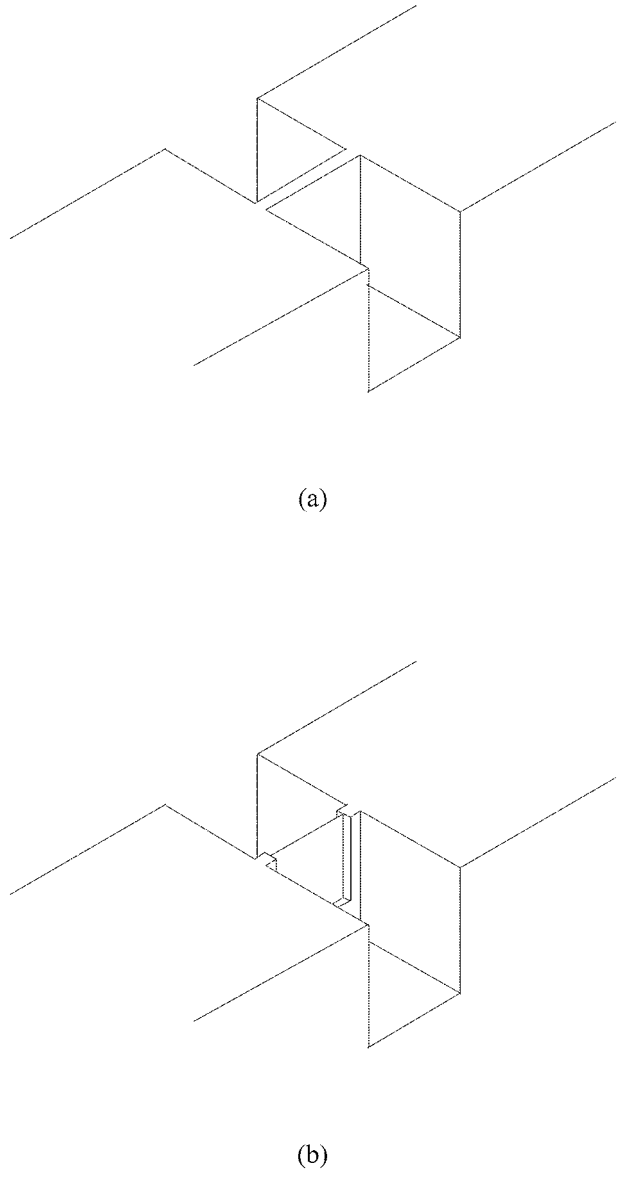

Figure 2 Schematic of FIB milling to create an electron transparent area: (a) after initial large mills; (b) after cleaning mills.

200 nm. Fig. 3 is a series of FIB images that visually show the milling steps. Fig. 3a shows a cross-section of the unmilled material (about 75 μm thick). Initial milling was performed using a large beam current (around 6.6 nA). This is achieved by inserting a large (∼500 μm diameter) beam-limiting aperture. Two mills about 10 μm wide, about 20–30 μm thick and to a depth of about 10 μm were performed to leave a thin strip of material about 1 μm in thickness in the starting material (Fig. 3b). The large aperture allows for rapid milling (about 1 hour per mill), however the milled surfaces are very rough and unsuitable for the TEM. This roughness is due not only to the broad diameter of this beam at the aperture size (∼300 nm), but also the effect of ion-induced channelling. Fig. 3c shows the milled cross-section tilted over to an angle of about 40° from the vertical. Away from the top surface rough vertical columns can be seen. These are artefacts associated with channelling of the ion beam at high beam current.

To remove the channelling artefacts and to reduce the thickness of the milled section to electron transparency,

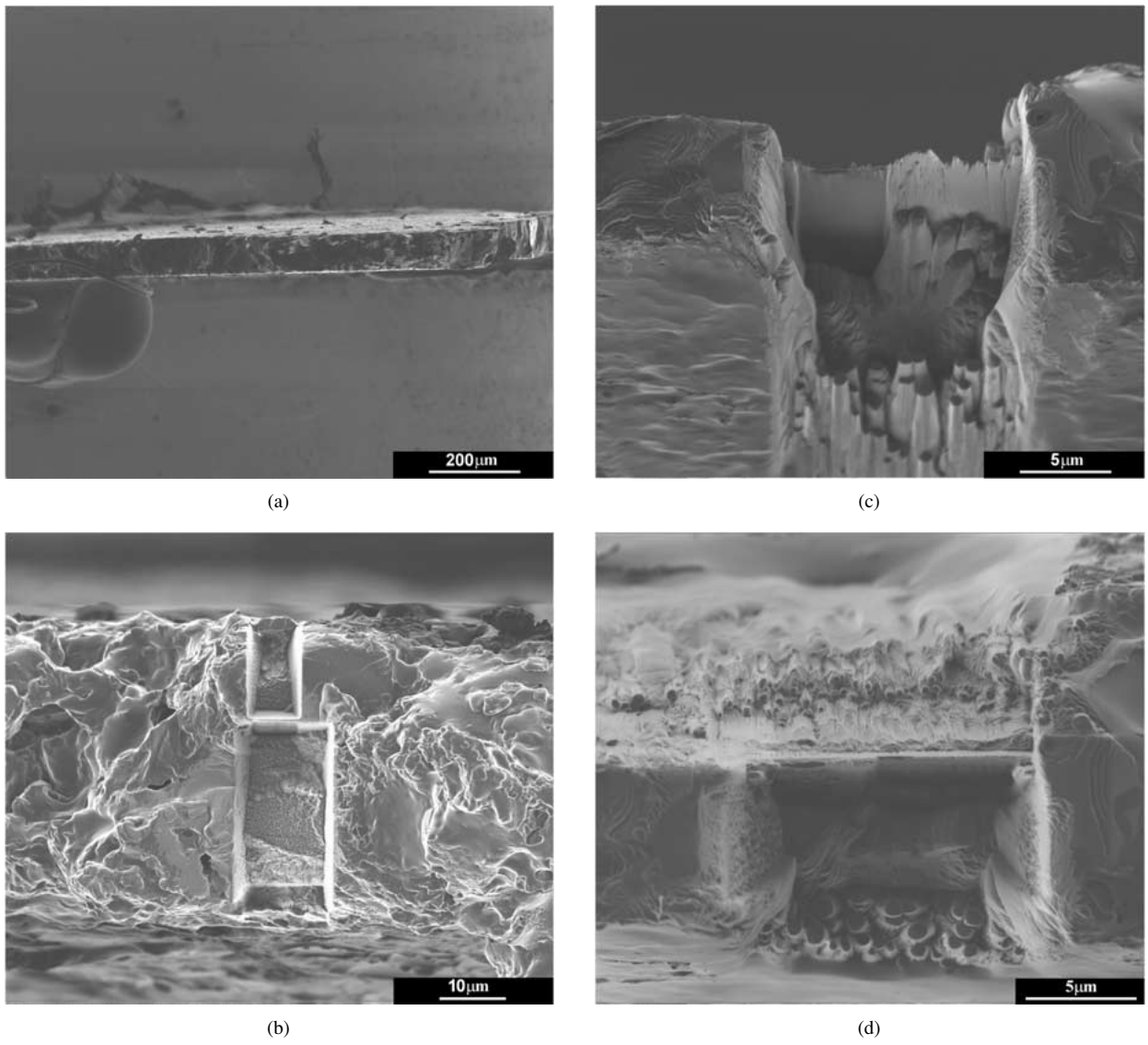

Figure 3 FIB images demonstrating the process of TEM specimen preparation. (a) Cross-section of the unmilled section. (b) Cross-section showing a 'H'-type initial milling. (c) Cross-section tilted by about 40° from the vertical showing the effect of the cleaning mill. (d) Cross-section of the finished specimen.

a series of cleaning mills were performed. These require a lower beam current (∼350 pA), obtained by inserting a smaller (200 μm diameter) beam-limiting aperture, and consist of a series of consecutive horizontal line mills progressing gradually into the unmilled strip. This milling is slower and more precise and not only leaves a smoother cross-section but also removes the channelling artefacts. This is shown in Fig. 3c, where the left hand side has been subject to a cleaning mill, whereas the right hand side has not. The left-hand side is clearly smoother and the artefacts have been removed. Cleaning mills were continued until the remaining region was about 100–200 nm thick (Fig. 3d). At this point, the sample was thin enough to be examined in the TEM.

Microstructural analysis and elemental mapping were carried out on a Philips CM200 FEG-STEM operating at 200 kV with an EDS detector attached.

3. Experimental methods

3.1. Resin impregnation method

A portion of $CuAl_2$ alloy was leached overnight as described above, then washed with water and followed by acetone before being placed in a resin. The resin used was "EpoThin" from Beuhler, chosen not only for its low viscosity and hence ability to penetrate the tiny pores, but also for its room temperature cure to avoid unnecessary heating which would alter the sensitive structure. Vacuum impregnating the resin protects the sample from aerial oxidation and also provides structural rigidity. The acetone wash assisted to draw the resin into the pores. The resin-impregnated sample was cut with a diamond saw, thinned on 1200 grit paper and milled as described above with the FIB. Although the resin penetrated the pores completely, holding the structure together and protecting it, the resin reacted under the energetic electron beam in the TEM, causing the sample to drift slightly, but sufficiently, during examination to make elemental mapping extremely difficult. Mapping times were typically 30 minutes and the features under examination were distributed over a scale of the order of a few nanometres.

3.2. Mill–Leach method

Because of the drift problem associated with the resin sample, a second sample was tried without resin. It was

decided to perform the milling on un-leached $CuAl_2$ alloy, then leach briefly before quickly placing the sample into the TEM. Two thin electron transparent areas were milled using the FIB. A conventional ∼100 nm thick region and a thicker (∼400 nm) region just in case the thinner region leached completely (likely since the structural ligaments were expected to be about 30 nm diameter). This sample was leached for about 20 minutes before washing and placing in the TEM. Unfortunately, both thinned regions leached completely and no electron transparent region remained.

3.3. Wedge Mill – Leach method

A similar method to "Mill - Leach", except the electron transparent region was milled in the shape of a wedge. The wedge consisted of an acute angle of about 5^0 and a length of about 5 μm. The principle was that some of the wedge would leach completely, however the thinnest possible region that could survive (hopefully being electron transparent) would be suitable for TEM analysis. Fig. 4 shows a FIB cross-section of a specimen milled to produce wedge-shaped sections. Two types of wedges are shown in this Figure. Firstly, on the left, a wedge-shaped region that decreases in thickness from right to left. Secondly, on the right, a wedge-shaped region that increases in thickness away from the top surface. This method gave the successful result for the zinc-doped material.

3.4. Leach-Mill method

Another method was tried, with the grit-paper thinned sample being leached for a few hours before milling with the FIB. This would ensure there was some thin leached region to view under the TEM. Following the FIB milling, the sample was stored under water until the TEM was available for use. Ethanol was used to wash the sample and allow quick drying before placing in the TEM. This method gave the successful result for the chromium-doped material.

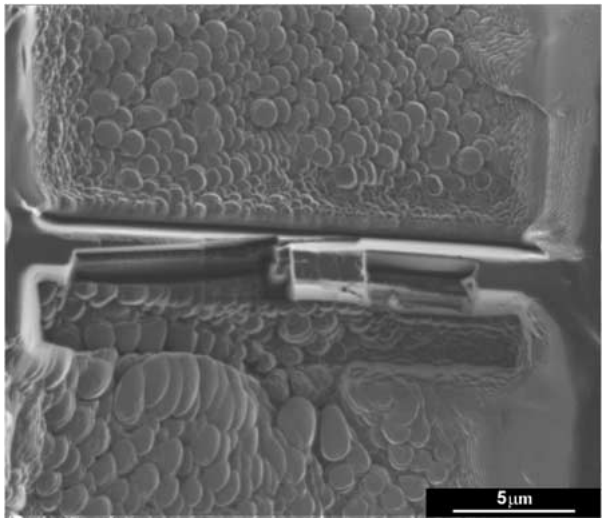

Figure 4 FIB image showing possible wedge-shaped sections suitable for TEM analysis. The wedge on the left decreases in thickness across the section from left to right and the wedge on the right increases in thickness away from the top surface.

4. Results

As already described, the resin reacted under the electron beam. Also, leaching after milling can completely remove electron transparent regions. The wedge mills worked however, and it was possible to obtain a very high magnification image of the doped skeletal copper as well as an elemental map of the position of zinc within the structure.

The high magnificiation images in Fig. 5 show a granulated structure for the zinc-doped skeletal copper, verifying the description of "agglomerated granules" suggested from x-ray diffraction results by Kalina *et al.* [10, 24]. These images also clearly show the ligament network structure as previously viewed directly by FIB examination [13, 16, 17] (Fig. 1). This is in contrast to the findings of Szot *et al.* [12] who claimed from TEM images of carbon replicas that the structure consisted of parallel curved rods of copper.

Fig. 6 shows a STEM image and zinc elemental map as well as an overlayed image of the two showing the

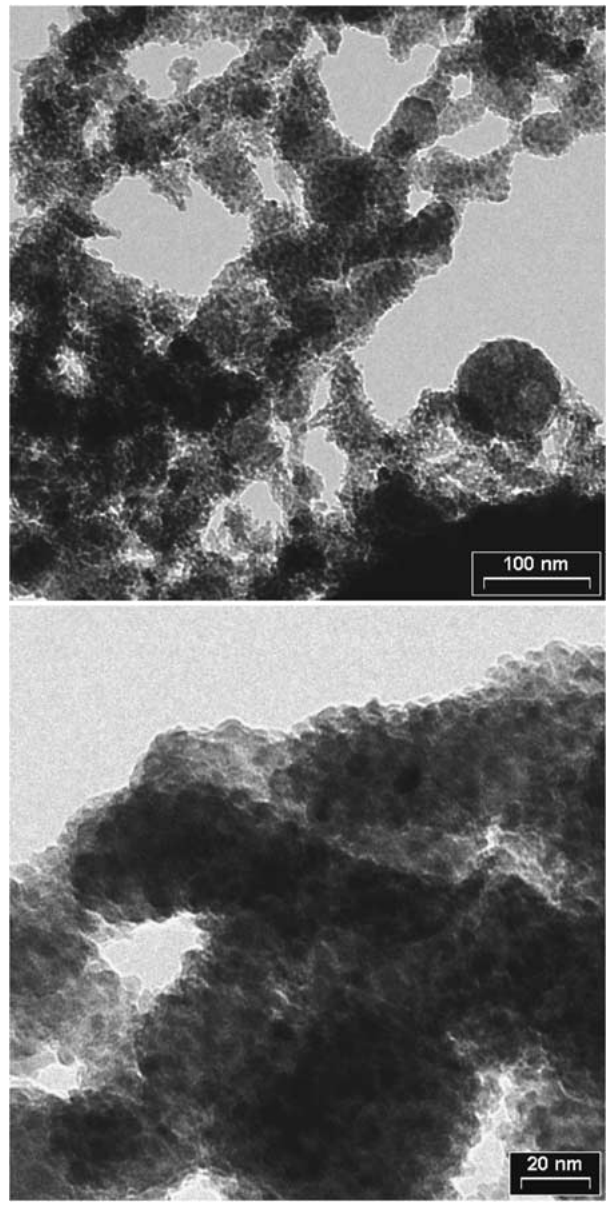

Figure 5 TEM images of zinc-doped skeletal copper at very high magnifications.

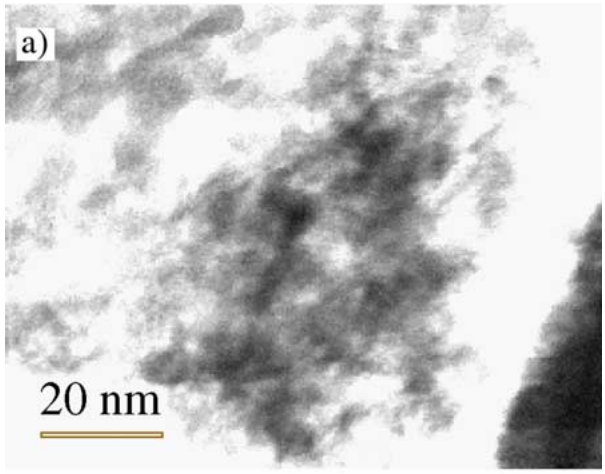

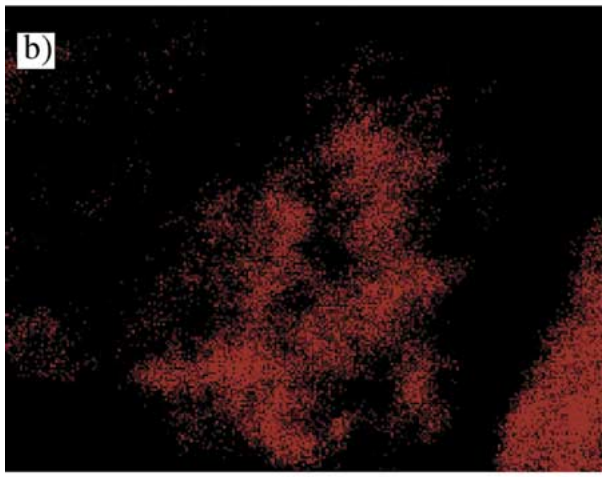

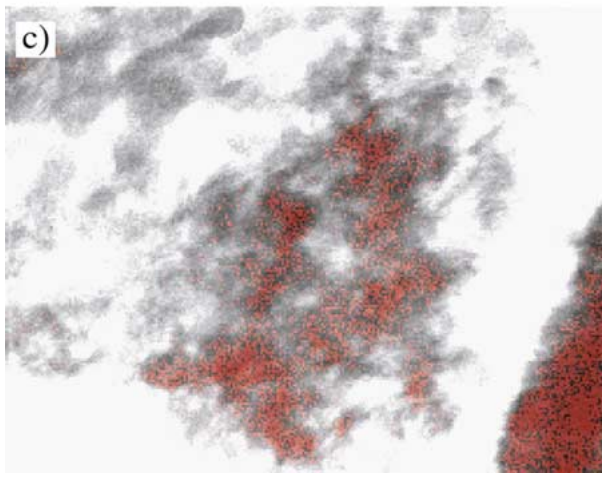

Figure 6 Elemental map for zinc location: (a) TEM electron image; (b) zinc signal map; (c) overlay of zinc and electron images.

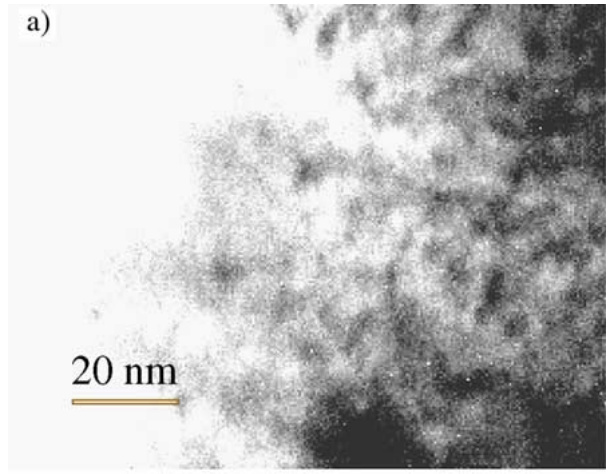

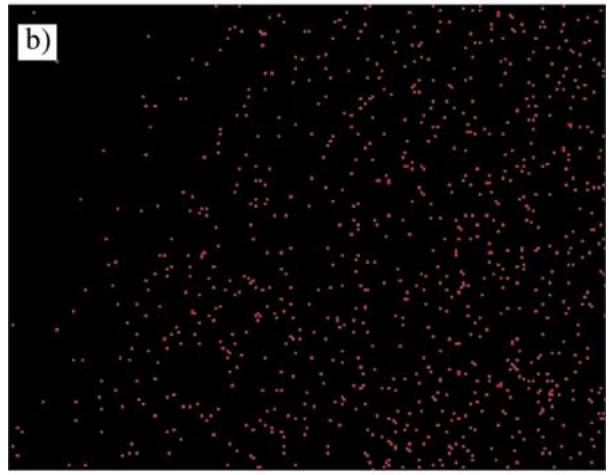

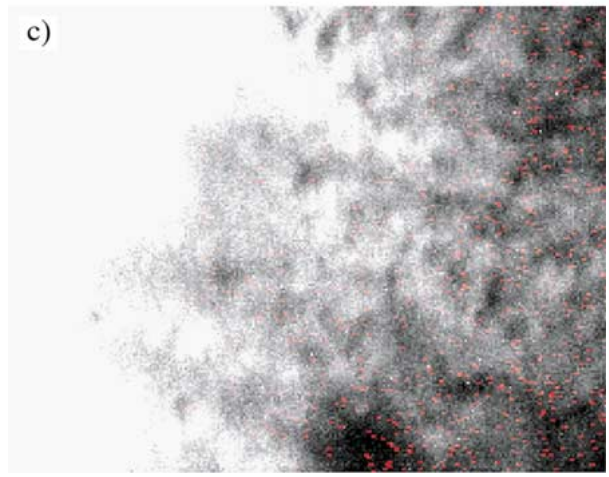

Figure 7 Elemental map for chromium location: (a) TEM electron image; (b) copper signal map; (c) overlay of chromium and electron images.

relative location of the zinc. It is clear that zinc resides primarily inside the copper ligaments. In contrast, chromium was found to reside on the outside of the ligaments (Fig. 7). The chromium elemental map shows a fairly even distribution of chromium across the image, with possibly only a slight increase in signal at the boundaries between the black shadows of the ligaments and the grey/white pore space. If the additive was located inside the ligaments, a distinct concentration would be seen in the middle of the black shadows, however only a weak signal is obtained in these regions, more characteristic of a surface deposit.

Aside from providing an improved knowledge of the structure of skeletal copper, the information given by the elemental maps in Figs 6 and 7 have also enabled a better understanding of the mechanisms involved during the leaching reaction [16, 17]. The differences between the chromium and zinc positions within the copper are indicative of the different mechanisms involved and the different ways in which they affect the overall copper structure. Chromium is deposited as Cr_2O_3 on the copper surface during leaching by electrochemical reduction from chromate. Its presence inhibits the copper dissolution/re-deposition

mechanism of rearrangement, thereby maintaining a very high surface area that would otherwise be reduced with time. Zinc, however, deposits as an oxide upon a drop in pH. The dissolution of aluminium at the reaction front consumes hydroxide, promoting the deposition of zinc oxide in this region. The zinc oxide becomes intimately mixed with the unstable copper at the leach front and is ultimately embedded in the ligaments that form. Most of the zinc oxide present on the outside of these ligaments re-dissolves after the leach front has passed and the pH rises to the bulk value again. However the zinc oxide trapped inside the copper ligaments remains, inhibiting the bulk diffusion of the copper atoms and thereby maintaining a high surface area. Since the zinc redissolves from the ligament surface, the dissolution/re-deposition of copper can still occur to a significant extent, and being the main mechanism of copper rearrangement, the surface area is ultimately still reduced with time in the presence of zinc.

Given the success of preparing skeletal copper for the TEM using the FIB in this way, it should be possible to analyse other skeletal catalysts (nickel, cobalt, etc.) in a similar way. This method may also lay the foundations of ways to prepare other porous and/or sensitive materials for the TEM that cannot be readily prepared using current conventional methods.

5. Conclusions

It has been shown that it is possible to create a TEM sample of a porous, sensitive material like doped skeletal copper by using the FIB. The TEM was able to image the sample at very high magnifications as well as provide elemental mapping showing where the additives lay with respect to the copper ligaments. In particular, the chromium was found to reside on the outside of the copper ligaments, whereas the zinc resided inside them. This information has provided a better understanding of the structure of skeletal copper as well as allowing a better analysis of the leaching mechanisms and how the additives affect the structure. The methods presented may provide the basis for TEM analysis of not only other skeletal catalysts but also other porous and/or sensitive materials.

Acknowledgements

Financial support from the Australian Research Council is gratefully acknowledged. AJS acknowledges receipt of an Australian Postgraduate Award. The authors would like to thank Robert Smith for his invaluable guidance in using the FIB for milling a thin section. Thanks also to Brian Cooper for the casting work and Dan O'Neil for assistance with resin vacuum impregnation.

References

1. L. FAUCOUNAU, *Bull. Soc. Chim.* **4**(5) (1937) 58 (Chem. Abs. 31:3217[1]).
2. A. D. TOMSETT, M. S. WAINWRIGHT, and D. J. YOUNG, *Appl. Catal.* **12** (1984) 43.
3. M. S. WAINWRIGHT, in "Handbook of Heterogeneous Catalysis," edited by G. Ertl, H. Knözinger and J. Weitkamp (1998) p. 64.
4. M. RANEY, *Ind. Eng. Chem.* **32**(9) (1940) 1199.
5. B. V. ALLER, *J. Appl. Chem.* **7** (1957) 130.
6. M. RANEY, US Patent no. 1, 563, 587 (Dec. 1, 1925).
7. *Idem.*, US Patent no. 1, 628, 190 (May 10, 1927).
8. L. M. KEFELI and S. L. LEL'CHUK, *Doklady Akad. Nauk S.S.S.R.* **84** (1952) 285 (Chem. Abs. 46:10822c).
9. *Idem.*, *Rentgen. Metody Issledovan. i Primenenie v Khim. Prom. Goskhimizdat* (Sbornik) (1953) 78 (Chem. Abs. 50:3862d).
10. M. M. KALINA, A. B. FASMAN and V. N. ERMOLAEV, *Deposited Doc. VINITI* **1022–80** (1980) 15 (Chem. Abs. 95:66291p).
11. U. BIRKENSTOCK, R. HOLM, B. REINFANDT and S. STORP, *J. Catal.* **93** (1985) 55.
12. J. SZOT, D. J. YOUNG, A. BOURDILLON and K. E. EASTERLING, *Phil. Mag. Lett.* **55**(3) (1987) 109.
13. A. J. SMITH, T. TRAN and M. S. WAINWRIGHT, *J. Appl. Electrochem.* **29**(9) (1999) 1085.
14. L. MA, D. L. TRIMM and M. S. WAINWRIGHT, in "Advances of Alcohol Fuels in the World" (Beijing, China, 1998) p. 1.
15. *Idem.*, *Topics in Catalysis* **8** (1999) 271.
16. A. J. SMITH, L. MA, T. TRAN and M. S. WAINWRIGHT, *J. Appl. Electrochem.* **30** (2000) 1097.
17. A. J. SMITH, T. TRAN and M. S. WAINWRIGHT, *ibid.* **30** (2000) 1103.
18. H. E. CURRY-HYDE, M. S. WAINWRIGHT and D. J. YOUNG, *Appl. Catal.* **77** (1991) 75.
19. L. MA, A. J. SMITH, T. TRAN and M. S. WAINWRIGHT, *Chem. Eng. Process.* **40** (2001) 59.
20. R. ANDERSON and S. J. KLEPEIS, in Specimen Preparation for Transmission Electron Microscopy of Materials IV, San Francisco, California, U.S.A., 1997 (Materials Research Society) Vol. 480, p. 187.
21. D. H.-I. SU, H. T. SHISHIDO, F. TSAI, L. LIANG and F. C. MERCADO, in Specimen Preparation for Transmission Electron Microscopy of Materials IV, San Francisco, California, U.S.A., 1997 (Materials Research Society) Vol. 480, p. 105.
22. M. W. PHANEUF, N. ROWLANDS, G. J. C. CARPENTER and G. SUNDARAM, in Specimen Preparation for Transmission Electron Microscopy of Materials IV, San Francisco, California, U.S.A., 1997 (Materials Research Society) Vol. 480, p. 39.
23. J. L. MURRAY, *Intern. Metals Rev.* **30**(5) (1985) 211.
24. M. M. KALINA, A. B. FASMAN and V. N. ERMOLAEV, *Kinet. Katal.* **21**(3) (1980) 813 (Chem. Abs. 93:81065v).

Received 28 March
and accepted 3 November 2000